Technical Notes

Measurement of Flame Transfer Functions in Swirl-Stabilized, Lean-Premixed Combustion

J. A. Ranalli,* C. R. Martin,† P. R. Black,‡
U. Vandsburger,§ and R. West¶
Virginia Polytechnic Institute and State University, Blacksburg, Virginia 24060

DOI: 10.2514/1.44187

Introduction

TO MEET increasingly stringent emission standards for nitric oxides, modern gas turbine designs use lean-premixed combustion. While meeting these new environmental standards, lean-premixed combustion systems introduce some substantial operability concerns with increased susceptibility to blowout, flashback, and instabilities. Significant effort is required to overcome these design challenges to allow turbines to operate in an efficient and environmentally friendly manner. This brief communication provides results of ongoing experimental measurements of lean-premixed combustion flame dynamics, necessary to further predictive capabilities of models for combustion instabilities. Measurements were made of linear flame transfer functions for both velocity and equivalence ratio oscillations. The flame transfer functions showed that the flame behaves as a low-pass filter for both types of excitation, but some important differences in the gain and cutoff frequency occurred. Although the gain and cutoff frequency both increased with equivalence ratio for velocity perturbations, they were observed to have no change with operating equivalence ratio for the case of equivalence ratio oscillations.

The types of combustion instabilities most commonly encountered in premixed combustion systems were first characterized by Rayleigh [1]. In this type of instability, a feedback loop is formed between the fluctuations in heat release rate (HRR) of the flame and the combustor/flow train acoustics [2,3]. Under certain operating conditions, the coupled system can become unstable, resulting in high-amplitude pressure fluctuations that can be detrimental to combustor hardware as well as efficiency. The specific coupling mechanisms by which these instabilities may arise are a significant area of research and readers are directed to the literature for a more significant discussion of the phenomenon [3,4].

For the purposes of this study, two possible mechanisms were considered [5,6]: coupling through velocity and equivalence ratio oscillations, as depicted in Fig. 1. Velocity (mass flow) coupling occurs when the acoustics directly cause a fluctuating mass flow upstream of the flame. The mechanism for equivalence ratio oscillations is known to be related to the injector design [7]. When considering a system level model of instabilities, knowledge of the flame and acoustic transfer functions is necessary to yield an understanding of the occurrence of instabilities [3].

Making useful predictions of instabilities using a closed-loop model, like the one described here, ultimately relies on component models to predict the individual transfer function blocks, of which the flame is the most difficult to characterize. The flame transfer function (FTF) represents the dynamics of the flame response to a perturbation as a function of frequency:

$$\mathrm{FTF}(f) = \frac{q'(f)}{u'(f)} \quad \text{or} \quad \frac{q'(f)}{\Phi'(f)}$$

This FTF may be expected to vary with the combustor operating condition and geometry. Previous modeling efforts have used a variety of physical models to attempt to predict these flame dynamics, including well-stirred reactor models [8,9] and, of more recent interest, flame sheet models [10–12]. Experimental measurements of flame dynamics have also been made by several investigators [13–20], though few considered flame response to equivalence ratio oscillations. The measurements made in this study provide an additional basis for the testing of flame dynamics models as well as offering insight into the flame physics.

The existing literature on velocity perturbations suggests that the flame acts as a low-pass filter in responding to excitations. Making accurate predictions of the flame dynamics thus relies on predicting the low-frequency gain and cutoff frequency of the FTF. Models show predictions of the low-frequency gain as tied to the mean energy content of the reacting mixture [8]. The bandwidth of the flame transfer function has been related to the nondimensional Strouhal number based on the flow convective time scales [12,14,19]. In dimensional terms, this corresponds to the hundreds of hertz range.

Experimental Setup and Procedure

Experiments were carried out on a rig specifically designed for gaseous, premixed, turbulent combustion experiments, as shown in Fig. 2. The rig design was a swirl-stabilized dump combustor with a center body. Swirl was generated by a fixed-vane swirler with vanes at a 30 deg angle to the flow axis. The actual combustion section was a quartz tube that vented to the atmosphere. The combustor section was sufficiently short as to prevent any self-excitation from occurring.

Mean air flow rates were fixed at 25 SCFM (0.0136 kg/s) for all tests in this study. Fuel flows were specified to provide mean equivalence ratios in the range of $\Phi = 0.48$–0.7 for both natural gas and propane. The low end of this range was bounded by the lean stabilization limit. The primary fuel/air mixing took place far upstream, eliminating the possibility of undesired equivalence ratio oscillations reaching the flame. Dynamic equivalence ratio oscillations were introduced through a separate fuel stream.

Because the combustor was not self-excited, it was necessary to deliberately introduce perturbations to the upstream flow rate and equivalence ratio. The flame output (i.e., HRR) was measured relative to each of these perturbations, resulting in the FTF. Excitation of each parameter occurred at a single frequency (sine dwell). This was done in 10 Hz intervals in the range of 10–400 Hz. Combining data

Received 6 March 2009; revision received 10 August 2009; accepted for publication 10 August 2009.

*Research Assistant, Virginia Active Combustion Control Group, Department of Mechanical Engineering, 114OPP Randolph Hall; jranalli@vt.edu. Student Member AIAA.

†Research Assistant, Virginia Active Combustion Control Group, Department of Mechanical Engineering, 114OPP Randolph Hall; chrisrm@vt.edu. Student Member AIAA.

‡Research Assistant, Department of Mechanical Engineering; currently Lord Corporation.

§Professor, Virginia Active Combustion Control Group, Department of Mechanical Engineering, 205 Randolph Hall; uri@vt.edu.

¶Professor, Virginia Active Combustion Control Group, Department of Mechanical Engineering, 204 Randolph Hall; westrl@vt.edu.

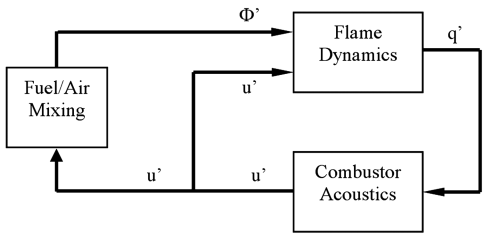

Fig. 1 System model of coupling that occurs in combustion instabilities.

from these single frequency excitations provided a full FTF over the entire frequency range of interest. The calibrated low-frequency gain (50 Hz) of the response was measured separately to prevent ambient variations from impacting the data. All data acquisition was performed using National Instruments hardware and software.

Dynamic Heat Release Rate Measurement

The output of the flame for both types of perturbation (i.e., the dynamic HRR) was measured using OH^* chemiluminescence, a common indicator of the flame HRR [21,22]. OH^* chemiluminescence was detected via a photomultiplier tube (PMT) with an optical bandpass filter centered at 308 nm. The PMT was mounted to detect incident radiation from the entire flame (global HRR). This integrated measurement was adequate to detect the fluctuations in heat release caused by the perturbation of interest, providing an accurate measure of the HRR response. This measurement was calibrated assuming complete combustion, yielding measurements in actual HRR units (kilowatts).

It has been noted by Lee and Santavicca [22] that care must be taken when using chemiluminescence as a dynamic HRR indicator due to nonlinearities in the baseline luminescence. This nonlinearity would serve to create an apparently elevated response magnitude for the case of equivalence ratio oscillations. In the present study, however, nonlinearity was not observed in the OH^* chemiluminescence calibration over the range of operating conditions considered. Thus, OH^* chemiluminescence serves as a suitable measure of oscillatory HRR in this range, even for the equivalence ratio oscillations.

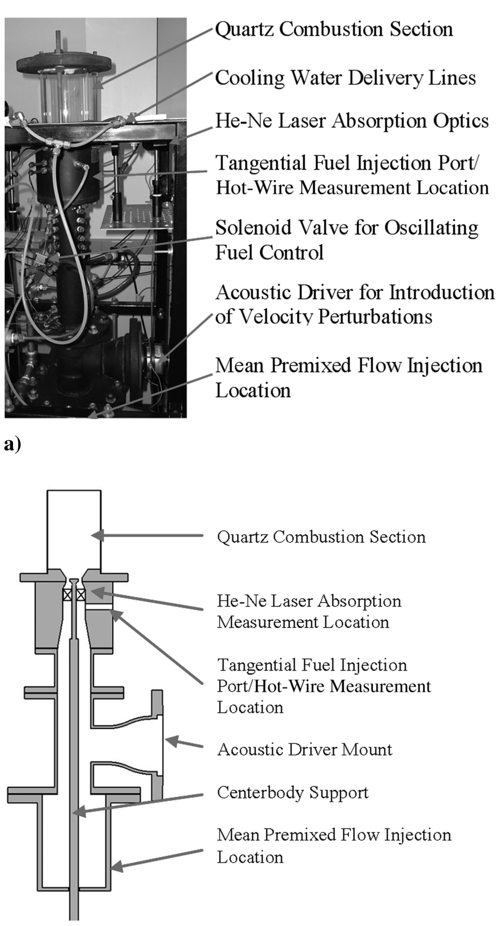

Fig. 2 Experimental apparatus a) photograph, b) sketch.

Dynamic Velocity Measurement

Perturbations in velocity were introduced by a speaker mounted on a side branch of the experimental apparatus (see Fig. 2). The power with which the speaker was excited was varied with frequency to ensure the highest transfer function coherence as possible, while remaining in the linear range of the OH^* chemiluminescence signal response. The linear range of the OH^* signal was assumed to be the range in which the second harmonic of the response had a magnitude 20 dB lower than that of the primary peak. The velocity oscillation amplitude reached a maximum of 13% of the mean flow rate, below the lowest (approximately 15%) limit for linearity in the response, as reported in literature [18,20]. Velocity perturbations were measured using a hot-wire anemometer directly upstream of the swirler. The hot wire was calibrated with an air jet to provide readings in meters per second.

Dynamic Equivalence Ratio Measurement

Perturbations in equivalence ratio were introduced using a solenoid valve, which delivered an additional fuel stream, injected radially, directly upstream of the swirler. The mean flow rate through this valve was varied such that resulting equivalence ratio oscillations had amplitude of approximately 5% of the overall fuel flow. These 5% oscillations in the overall fuel flow rate comprised, at most, 0.3% oscillations of the total mass flow rate. For the mass flow rate (velocity) oscillations, the oscillation level required to yield a coherent response was between 2 and 13% of the mean. Thus, these incidental mass flow oscillations due to the additional fuel injection may be considered to be negligible. FTF coherence remained high (>0.9) for the equivalence ratio perturbation measurements out to the limit of excitation (400 Hz), indicating sufficient bandwidth in the solenoid valve to provide excitation at these frequencies.

The dynamic equivalence ratio caused by this fluctuating fuel flow was measured using absorption of a He–Ne laser at 3.39 μm. The laser beam was split onto a photodiode before passing through the flow to measure a reference power level. The remaining beam passed through the flow and the attenuated beam intensity was detected by a second photodiode. This absorption measurement, in combination with an absorption coefficient, yields a measurement of fluctuating fuel mole fraction, which was then used to calculate the fluctuating equivalence ratio. Absorption coefficients for the fuels used in this study were obtained from existing literature [23,24].

Data Acquired

In the case of velocity perturbations, full frequency response plots were measured over the equivalence ratio range of lean blowout (around $\Phi = 0.50$) through $\Phi = 0.70$. The results for these tests were measured for natural gas and propane and are shown here in Figs. 3 and 4, respectively. The leanest case was fixed by the lean limit for blowoff for the fuel in this combustor. Results for the leanest conditions showed higher scatter and lower coherence due to the reduced overall flame heat release and intrinsic fluctuations present as blowoff was approached.

FTF measurements for equivalence ratio perturbations were conducted on both natural gas and propane for mean equivalence ratios from the lean extinction limit up to $\Phi = 0.70$. These test results are presented in Figs. 5 and 6, respectively. As with the velocity tests, the leanest test conditions exhibit a reduced coherence due to the reduction in overall HRR and increase in inherent unsteadiness in the flame.

All of the data presented here are in appropriate calibrated units for the perturbation of interest. In the case of response of HRR to velocity perturbations, this is kilowatts per meters per second, whereas, for

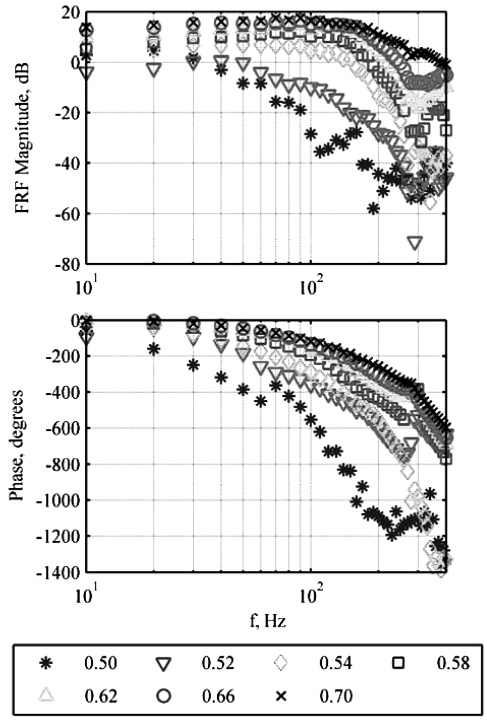

Fig. 3 Response of flame HRR to velocity perturbations for natural gas.

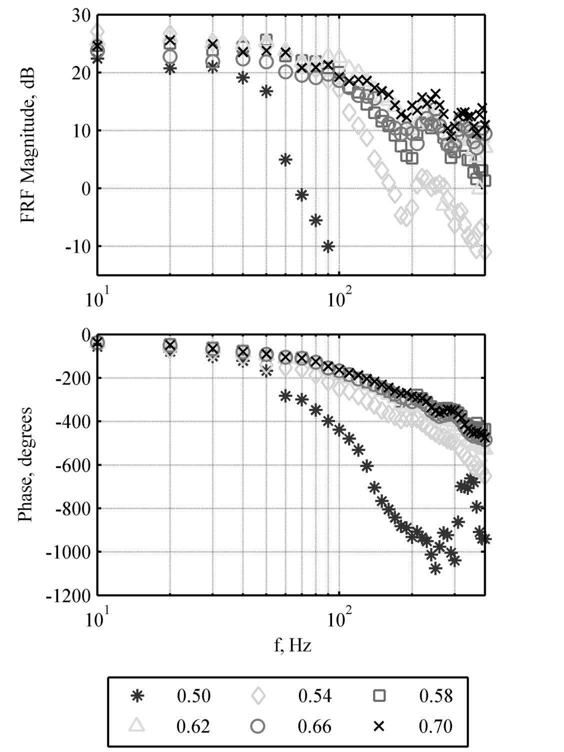

Fig. 5 Response of flame HRR to equivalence ratio perturbations for natural gas.

response of HRR to equivalence ratio perturbations, the units are kilowatts per Phi. The method by which these calibrated units were obtained is discussed in the pertinent preceding sections.

The response of the flame to both types of perturbations exhibits behavior similar to that of a low-pass filter, namely, it is constant up to the bandwidth, after which the magnitude of the response is damped. Trends in low-frequency gain and bandwidth are presented here in Fig. 7 to provide a picture of how varying equivalence ratio and fuel choice affects the characteristics of this low-pass filter behavior. Bandwidth was measured at the point of 5 dB of drop from the low-frequency level. The low-frequency gains for perturbations in velocity show a rising trend with increasing equivalence ratio, whereas the gain for equivalence ratio perturbations is nearly constant except at the leanest cases. The equivalence ratio perturbation bandwidths shown in Fig. 7 also exhibit a predominantly constant trend, except in those cases closest to blowoff. Additionally, trends for a given type of perturbation agree well between the two fuels. The

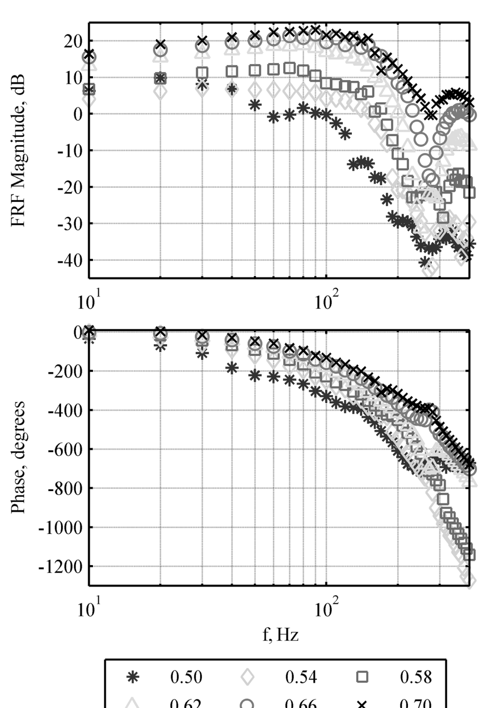

Fig. 4 Response of flame HRR to velocity perturbations for propane.

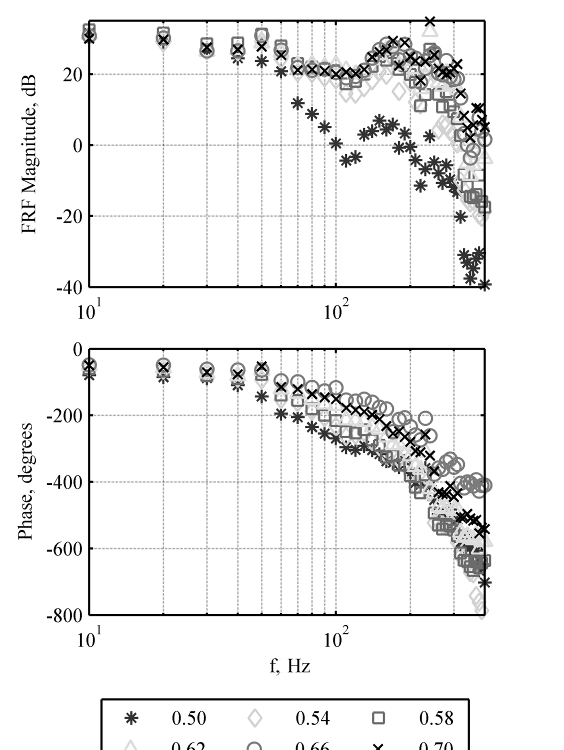

Fig. 6 Response of flame HRR to equivalence ratio perturbations for propane.

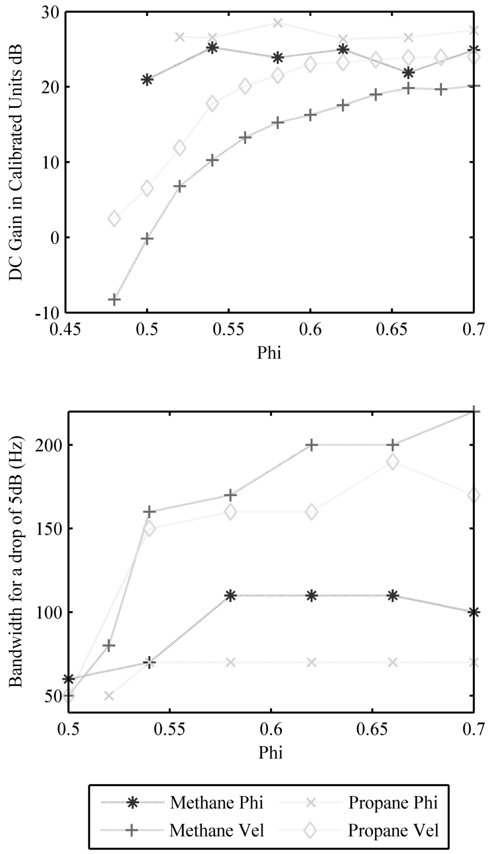

Fig. 7 Bandwidth and low-frequency (dc) gain compiled from all test cases.

linear character of the FTF phase indicates some time delay between the input and the response. This time delay, calculated based on the rate of change of phase at low frequency, is plotted as a function of equivalence ratio for each test case in Fig. 8. The delay exhibits a decreasing trend with increasing equivalence ratio.

Measurements of flame dynamic response to both velocity and equivalence ratio perturbations showed similar flame behavior. The measurements of velocity perturbations (Figs. 3 and 4) made in this study were in agreement with those already found in literature. Dynamic time scales of the cutoff frequency were on the order of milliseconds, the same order as fluid mechanical phenomena. Further, although quantitative measurements of the flame size were not available for this brief communication, qualitative observations agreed with expectations, with decreases in equivalence ratio resulting in an elongated flame. Variation of cutoff frequency with operating condition exhibited trends consistent with the argument

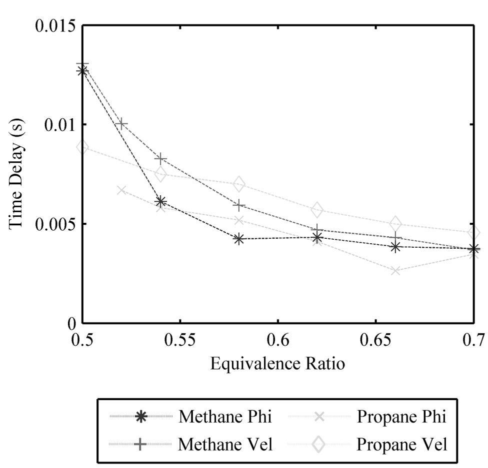

Fig. 8 Time delay compiled for all test cases.

that the dynamics are governed by convection of coherent flow structures to the flame for both fuels. Phase was predominantly linear and was on the order of milliseconds, corresponding approximately to convective time scales for this combustor. Time delay is observed to increase with decreasing equivalence ratio, consistent with expectations based on the relationship between convection and flame length. However, because only global chemiluminescence measurements were made, nondimensionalization of the frequency to Strouhal number is not possible for this data.

Conclusions

Velocity FTF bandwidths decreased with decreasing equivalence ratio, consistent with the trend discussed in literature. For equivalence ratio perturbations (Figs. 5 and 6), bandwidths remained in the range of hundreds of hertz, but occurred at constant frequency excepting the leanest conditions considered. Low-frequency gain exhibited an increasing trend with respect to mean equivalence ratio for the case of velocity perturbations, but remained practically constant for the case of equivalence ratio perturbations. These behaviors were consistent for both fuels. Time delay in the phase was still observed to be on the order of milliseconds, again corresponding to convective time scales. Overall, time delay was slightly shorter for equivalence ratio perturbations, however, no significant variation in the delay is observed between fuels. This behavior may be explained due to the fact that the laser absorption measurement was located slightly downstream of the hot wire, leading to a smaller expected value for convection time between these two locations.

The implications of the FTF characteristics on the expected behavior of system stability are as follows. Because the acoustic transfer function of a combustor remains nominally constant with respect to operating condition, the changes in flame transfer function characteristics would be expected to be most important in instability predictions. Increases in both the overall gain and flame transfer function bandwidth should therefore lead to a higher predicted incidence of instabilities. For the case of velocity perturbations, instability would be expected to be more common with increasing equivalence ratio on both counts.

For both types of perturbation, phase delay nominally increased with decreasing equivalence ratio. Thus, phase crossings will shift to lower frequencies, where the response has not yet rolled off. For the case of instability driven by equivalence ratio oscillations, where bandwidth and gain did not vary with equivalence ratio, decreasing equivalence ratio shows predicted potential for instabilities due to this phase behavior. All of these predictions should be taken with the important caveat that the combination of the FTF with the acoustic transfer function is necessary to fully ascertain the response.

Future work in this area needs to continue to experiment across a broader range of fuels to completely validate the predicted behavior of the flame frequency response function. Further, the spatial characteristics of the flame need to be considered by applying two-dimensional heat release. Continued work is also planned to consider the response of the flame size to the perturbations of interest to facilitate future modeling efforts. Finally, flame transfer function behavior offers potential insights into the expected instability behavior of the combustor, but practical application of these predictions should be tested against unstable combustion operating maps for validation.

Acknowledgments

The authors acknowledge the financial support of the Department of Energy through the University Turbine Research Program and the South Carolina Institute of Energy Studies. Author J. Ranalli would also like to thank the U.S. Department of Defense for funding through the National Defense Science and Engineering Graduate Fellowship.

References

[1] Rayleigh, J., *The Theory of Sound*, 2nd ed., Dover, New York, 1945.
[2] Sattelmayer, T., and Polifke, W., "Assessment of Methods for the

Computation of the Linear Stability of Combustors," *Combustion Science and Technology*, Vol. 175, No. 3, 2003, pp. 453–476. doi:10.1080/00102200302382

[3] Lieuwen, T. C., and Yang, V. (eds.), "*Combustion Instabilities in Gas Turbine Engines: Operational Experience, Fundamental Mechanisms, and Modeling*," Vol. 210, Progress in Astronautics and Aeronautics, AIAA, Reston, VA, 2005, p. 657.

[4] Huang, Y., and Yang, V., "Dynamics and Stability of Lean-Premixed Swirl-Stabilized Combustion," *Progress in Energy and Combustion Science*, Vol. 35, No. 4, 2009, pp. 293–364. doi:10.1016/j.pecs.2009.01.002

[5] Schildmacher, K., Koch, R., and Bauer, H., "Experimental Characterization of Premixed Flame Instabilities of a Model Gas Turbine Burner," *Flow, Turbulence and Combustion*, Vol. 76, No. 2, 2006, pp. 177–197. doi:10.1007/s10494-006-9012-z

[6] Lieuwen, T., Neumeier, Y., and Zinn, B., "Role of Unmixedness and Chemical Kinetics in Driving Combustion Instabilities in Lean Premixed Combustors," *Combustion Science and Technology*, Vol. 135, Nos. 1–6, 1998, pp. 193–211. doi:10.1080/00102209808924157

[7] Venkataraman, K. K., Preston, L. H., Simons, D. W., Lee, B. J., Lee, J. G., and Santavicca, D. A., "Mechanism of Combustion Instability in a Lean Premixed Dump Combustor," *Journal of Propulsion and Power*, Vol. 15, No. 6, 1999, pp. 909–918. doi:10.2514/2.5515

[8] Martin, C., "Systematic Prediction and Parametric Characterization of Thermo-Acoustic Instabilities in Premixed Gas Turbine Combustors," M.S. Thesis, Dept. of Mechanical Engineering, Virginia Technological and State University, Blacksburg, VA, Sept. 2006.

[9] Park, S., Annaswamy, A., and Ghoniem, A., "Heat Release Dynamics Modeling of Kinetically Controlled Burning," *Combustion and Flame*, Vol. 128, No. 3, 2002, pp. 217–231. doi:10.1016/S0010-2180(01)00347-9

[10] Preetham, Hemchandra, S., and Lieuwen, T., "Dynamics of Laminar Flames Forced by Harmonic Velocity Disturbances," *Journal of Propulsion and Power*, Vol. 24, No. 6, 2008, pp. 1390–1402. doi:10.2514/1.35432

[11] Dowling, A., "A Kinematic Model of a Ducted Flame," *Journal of Fluid Mechanics*, Vol. 394, No. 1, 1999, pp. 51–72. doi:10.1017/S0022112099005686

[12] You, D., Huang, Y., and Yang, V., "A Generalized Model of Acoustic Response of Turbulent Premixed Flame and its Application to Gas-Turbine Combustion Instability Analysis," *Combustion Science and Technology*, Vol. 177, Nos. 5–6, 2005, pp. 1109–1150. doi:10.1080/00102200590927012

[13] Hendricks, A. G., and Vandsburger, U., "The Effect of Fuel Composition on Flame Dynamics," *Experimental Thermal and Fluid Science*, Vol. 32, No. 1, 2007, pp. 126–132. doi:10.1016/j.expthermflusci.2007.02.007

[14] Lohrmann, M., and Buchner, H., "Prediction of Stability Limits for LP and LPP Gas Turbine Combustors," *Combustion Science and Technology*, Vol. 177, No. 12, 2005, pp. 2243–2273. doi:10.1080/00102200500241040

[15] Paschereit, C., Schuermans, B., Polifke, W., and Mattson, O., "Measurement of Transfer Matrices and Source Terms of Premixed Flames," *Journal of Engineering for Gas Turbines and Power*, Vol. 124, No. 2, 2002, pp. 239–247. doi:10.1115/1.1383255

[16] Durox, D., Schuller, T., and Candel, S., "Combustion Dynamics of Inverted Conical Flames," *Proceedings of the Combustion Institute*, Vol. 30, No. 2, 2005, pp. 1717–1724. doi:10.1016/j.proci.2004.08.067

[17] Balachandran, R., Dowling, A. P., and Mastorakos, E., "Non-Linear Response of Turbulent Premixed Flames to Imposed Inlet Velocity Oscillations of Two Frequencies," *Flow, Turbulence and Combustion*, Vol. 80, No. 4, 2008, pp. 455–487. doi:10.1007/s10494-008-9139-1

[18] Balachandran, R., Ayoola, B. O., Kaminski, C. F., Dowling, A. P., and Mastorakos, E., "Experimental Investigation of the Non-Linear Response of Turbulent Premixed Flames to Imposed Inlet Velocity Oscillations," *Combustion and Flame*, Vol. 143, Nos. 1–2, 2005, pp. 37–55. doi:10.1016/j.combustflame.2005.04.009

[19] Kim, T. K., Lee, J. G., Hyung, J. L., Quay, B. D., and Santavicca, D., "Characterization of Forced Flame Response of Swirl-Stabilized Turbulent Lean-Premixed Flames in a Gas Turbine Combustor," *Proceedings of the ASME Turbo Expo 2009: Power for Land, Sea and Air*, GT 2009-60031, American Society of Mechanical Engineers, Fairfield, NJ, 2009, p. 9.

[20] Bellows, B. D., Neumeier, Y., and Lieuwen, T., "Forced Response of a Swirling, Premixed Flame to Flow Disturbances," *Journal of Propulsion and Power*, Vol. 22, No. 5, 2006, pp. 1075–1084. doi:10.2514/1.17426

[21] Haber, L., and Vandsburger, U., "A Global Reaction Model for OH^* Chemiluminescence Applied to a Laminar Flat-Flame Burner," *Combustion Science and Technology*, Vol. 175, No. 10, 2003, pp. 1859–1891. doi:10.1080/713713115

[22] Lee, J. G., and Santavicca, D. A., "Experimental Diagnostics for the Study of Combustion Instabilities in Lean Premixed Combustors," *Journal of Propulsion and Power*, Vol. 19, No. 5, 2003, pp. 735–750. doi:10.2514/2.6191

[23] Tsuboi, K., Inomata, K., Tsunoda, Y., Isobe, A., and Nagaya, K., "Light Absorption by Hydrocarbon Molecules at 3.392 μm of He-Ne Laser," *Japanese Journal of Applied Physics*, Vol. 24, Pt. 1, 1985, pp. 8–13. doi:10.1143/JJAP.24.8

[24] Perrin, M., and Hartmann, J., "High Temperature Absorption of the 3.39 μm He-Ne Laser Line by Methane," *Journal of Quantitative Spectroscopy and Radiative Transfer*, Vol. 42, No. 6, 1989, pp. 459–464. doi:10.1016/0022-4073(89)90036-8

T. Lieuwen
Associate Editor